Status of Q5 Milestones & Progress Report at BNL Magnet Division

Ramesh Gupta, S. Lakshmi Lalitha and Piyush Joshi
(For Superconducting Magnet Division)

Summary

Work performed during 5th Quarter is summarized below:

- Overall SMES coil design completed with the basic coil structure for Q6 Go/NoGo milestone defined
- Magnetic and mechanical analysis of 10^{+} T Q6 structure completed
- Mechanical analysis for preliminary structure of ~24 T SMES coil started with ANSYS
- Coil winding machine upgrade completed with improved control on winding tension and to wind each coil in a significantly less time than in the previous system
- Four pancakes coils for the inner layer wound
- Fixture to perform 77 K QA test of two pancake coils plus splice joint built
- Two types of splice joint for constructing coil to satisfy Q6 Go/NoGo milestone built and tested
- Basic quench protection system built and tested before developing a full scale system to protect a large number of pancake coils in the Q6 Go/NoGo milestone

Superconducting Magnet Division does not have any Q5 milestone. Please see more details of the above ongoing tasks in following pages.

Progress Report

Overall SMES Coil Design

The overall design of SMES coil consists of inner and outer layers with each containing a number of pancake coils in them. An intermediate support structure between the inner and the outer layers is incorporated to keep stress and strain within the coil below a limit so that the performance is not significantly degraded. In the previous version of the design each pancake consisted of inner and outer coils with a split in the support structure to allow conductor to go from inner to outer layer in a complex geometry (see Fig.1 left). This required significant engineering. Moreover, since the inner and outer pancakes are wound separately, splice joint was required to be placed in the transition region of each inner and outer pancake.

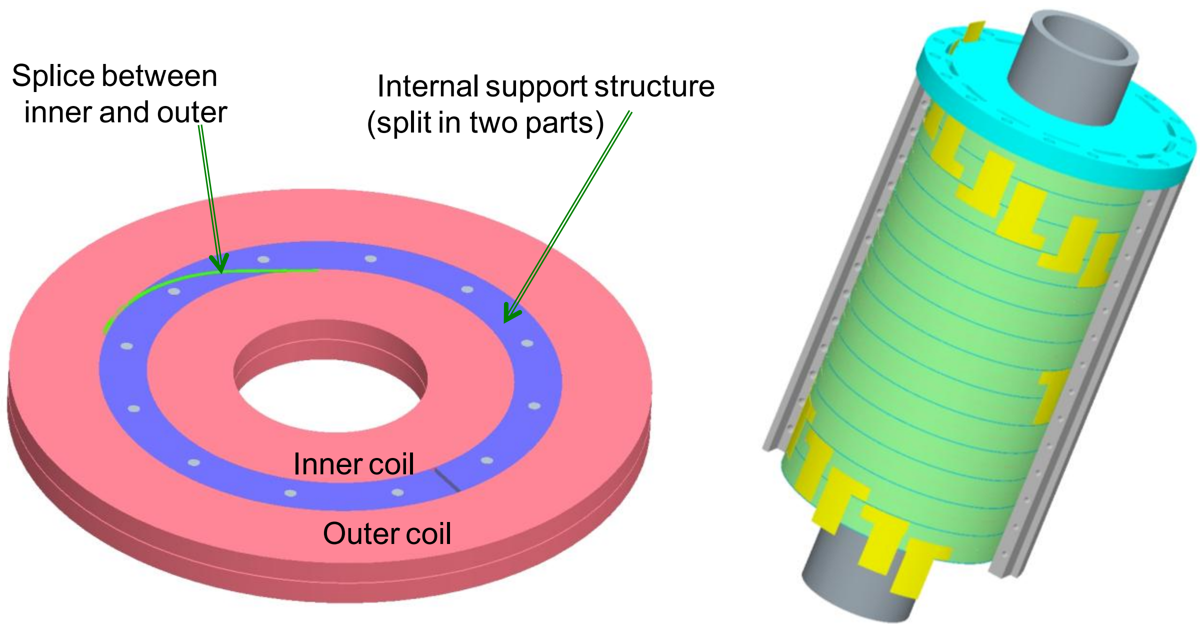

Fig. 1: Left side shows the previous design of internal structure (outer structure is not shown) with inner and outer coils and right side shows current structure for inner coil (end sections not shown for clarity).

We have significantly simplified the above design by placing inner and outer coils in their own independent support structures. Thus, a common structure will enclose all inner coils (see Fig. 2 right) for inner coil package in its own support structure. For clarity two end sections with a separate support structure are not shown in the figure. Fig. 1 (right) also shows a conceptual design with a number of leads (yellow in Fig. 1 right) brought out to help extract energy from small sections of coil rather than from the coil as a whole (which would be a large amount). The actual number of leads to be brought out will depend on the the amount of energy that can be deposited in a group of coils. These leads and the coils will be eventually connected externally with the overall SMES system to be energized only by a pair of leads.

Magnetic Design of Q6 Go/NoGo Structure

The magnetic design of the Q6 Go/NoGo structure is updated to meet the design approach discussed in previous section. The minimum required field to be achieved in Q6 structure is 10 T which will now be achieved with six or more double pancake coils being built for the inner layers. The earlier design was based on two double pancake coils each for inner and outer. The two cases are shown in Fig. 2 with the previous structure displayed on left and the current on right. Both cases used the same amount of conductor (600 meter). The magnitude of the field is superimposed on the geometry at the design current of SMES coil.

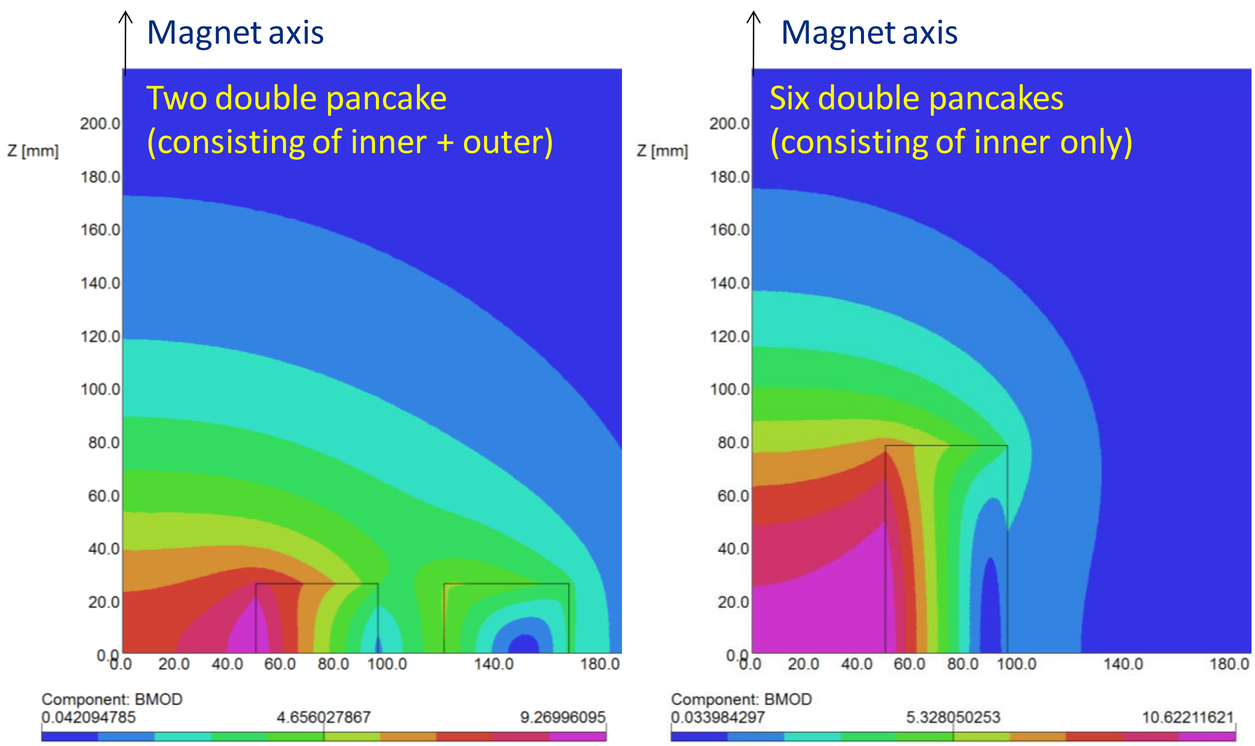

Fig. 2: Left side shows the field contour and coil of previous Go/NoGo structure consisting of inner and outer coils and right side shows the current structure consisting of only inner coil (only upper half of the 2-d axis symmetry model is displayed).

Mechanical Structure Analysis

2-d mechanical analysis of Q6 Go/NoGo structure has been carried out with the code ANSYS for the cases when the support structure is made with stainless steel or with Aluminum. The first case represents the part of intermediate stainless steel structure between inner and outer coils of the final higher field (~24 T) SMES design and the second case is the simpler Aluminum structure that is sufficient to contain the smaller magnitude of Lorentz forces associated with the smaller lower field (~10 T) Q6 structure. These calculations are based on the currently available mechanical properties (see Table 1) and do not yet include thermal effects. These calculations will be updated when they become available for the present conductor. The mechanical analysis is performed for seven double pancakes (rather than six), to include the possibility of more pancakes becoming available than the minimum desired.

Table 1: Material properties used in performing the mechanical analysis

MATERIAL	MECHANICAL PROPERTIES (For Structural analysis)	
SS	Young's Modulus (isotropic)	200 GPa
	Yield Strength	250 MPa
	Ultimate tensile Strength	460 MPa
	Poisson's Ratio	0.3
Al	Young's Modulus (isotropic)	71 GPa
	Yield Strength	280 MPa
	Ultimate tensile Strength	310 MPa
	Poisson's Ratio	0.33
HTS	Youngs Modulus (orthotropic) In-plane Out-of-plane	 122 GPa 68 GPa
	Shear Modulus	47 GPa
	Poisson's Ratio	0.3
Air	Young's Modulus	1.68e+5 Pa
	Poisson's Ratio	0.33

Fig. 3 shows the deformation in the whole magnet assembly for 25 mm thick radial outer structure made of either stainless steel (left side) or Aluminum (right side). Fig. 4 shows the equivalent stresses in the whole magnet. Fig. 5 shows the equivalent strains in the HTS coil to ensure that they remain below the acceptable limit. Since the values are acceptable for both Aluminum and stainless steel structure, for expediency and cost, we might use a simpler Aluminum structure to meet Q6 goal.

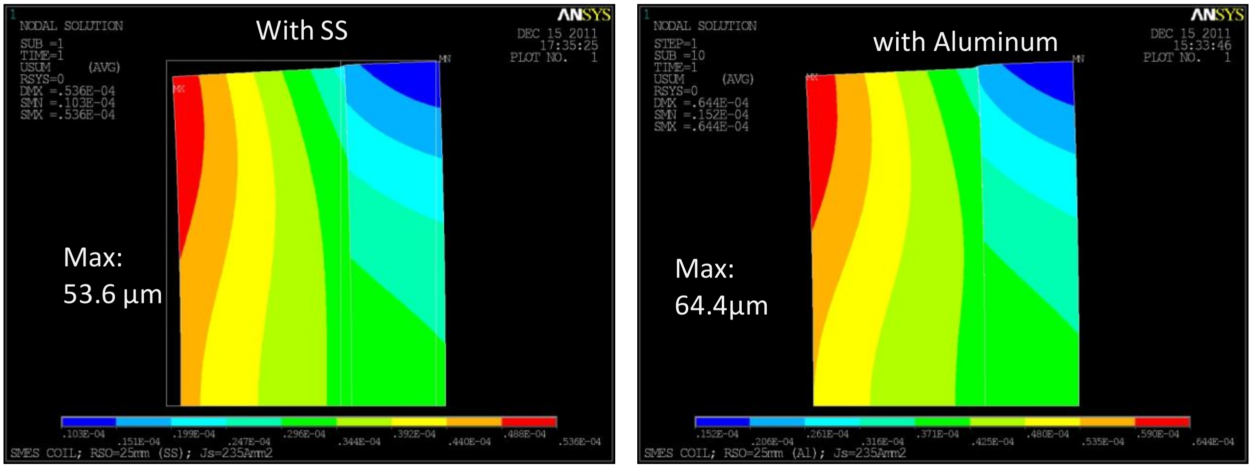

Fig. 3: Computed deformation for the 25 mm radial structure made with stainless steel (left side) and Aluminum (right side). Only upper half of the 2-d axis symmetry ANSYS model is displayed.

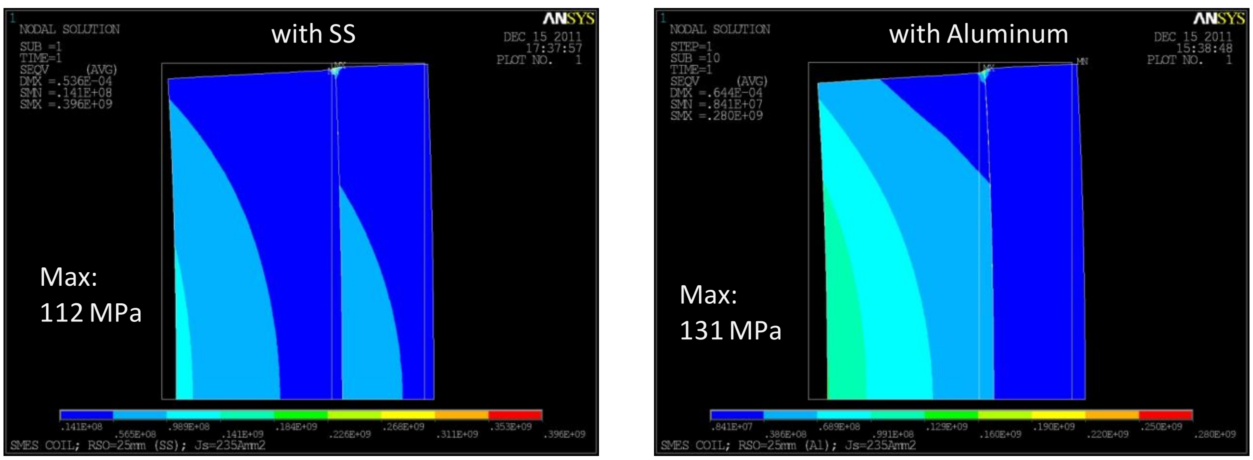

Fig. 4: Computed stresses for structure made with stainless steel (left side) and Aluminum (right side).

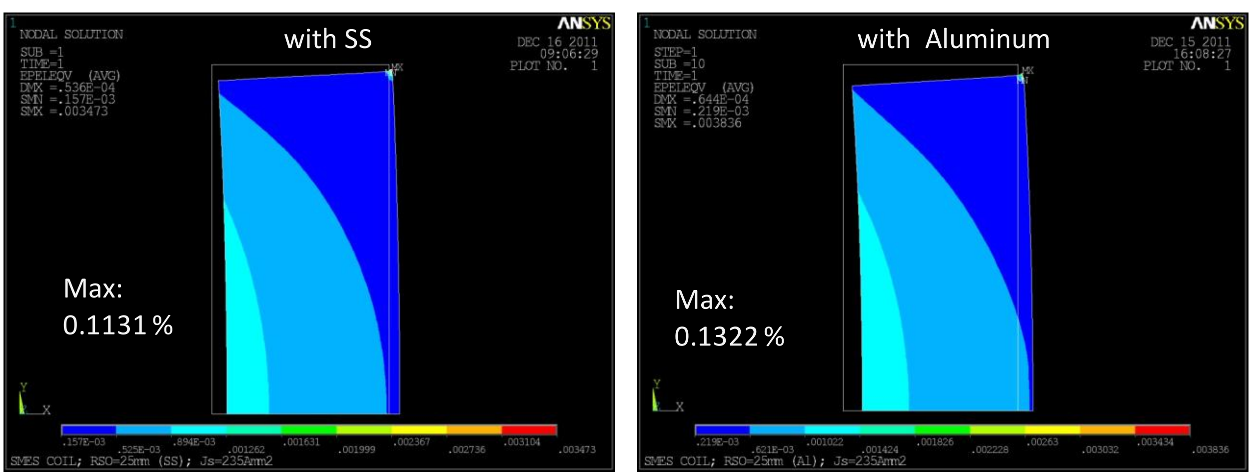

Fig. 5: Computed equivalent strain in HTS coils for structure made with stainless steel (left side) and Aluminum (right side).

Construction

Experience from winding of three mini pancake HTS test coils in previous quarter made it clear that the winding machine needs to be updated to provide better control on the tension and to reduce time required in winding each coil. The logic of winding machine was changed in the updated tooling so that the part that was fixed became rotating and the part that was moving became fixed (see Fig. 6 left). This significantly reduced the winding time for each coil from several days to one day. This upgrade also eliminated the steps which had potential for loosing part of the tension during winding. Moreover, the tension controller itself was replaced with the one that is more appropriate for this application.

A full size inner pancake coil wound with the updated machine is shown in Fig. 6 (right). The bottom right part in Fig. 6 shows the side of the coil with a number of voltage tap installed for diagnostics and the top part the other side as it will be in the final SMES coil package. We have completed winding four such pancake coils so far. Each coil uses 100 meter of 12 mm wide HTS tape.

We have also constructed a fixture to test a double pancake coil module at 77 K in liquid nitrogen. Such measurements serve as the basic QA tests as we have found that most potential degradation and/or possible defects can be detected at 77 K without risking the whole coil which must be tested at 4 K in liquid helium in a much more expensive test.

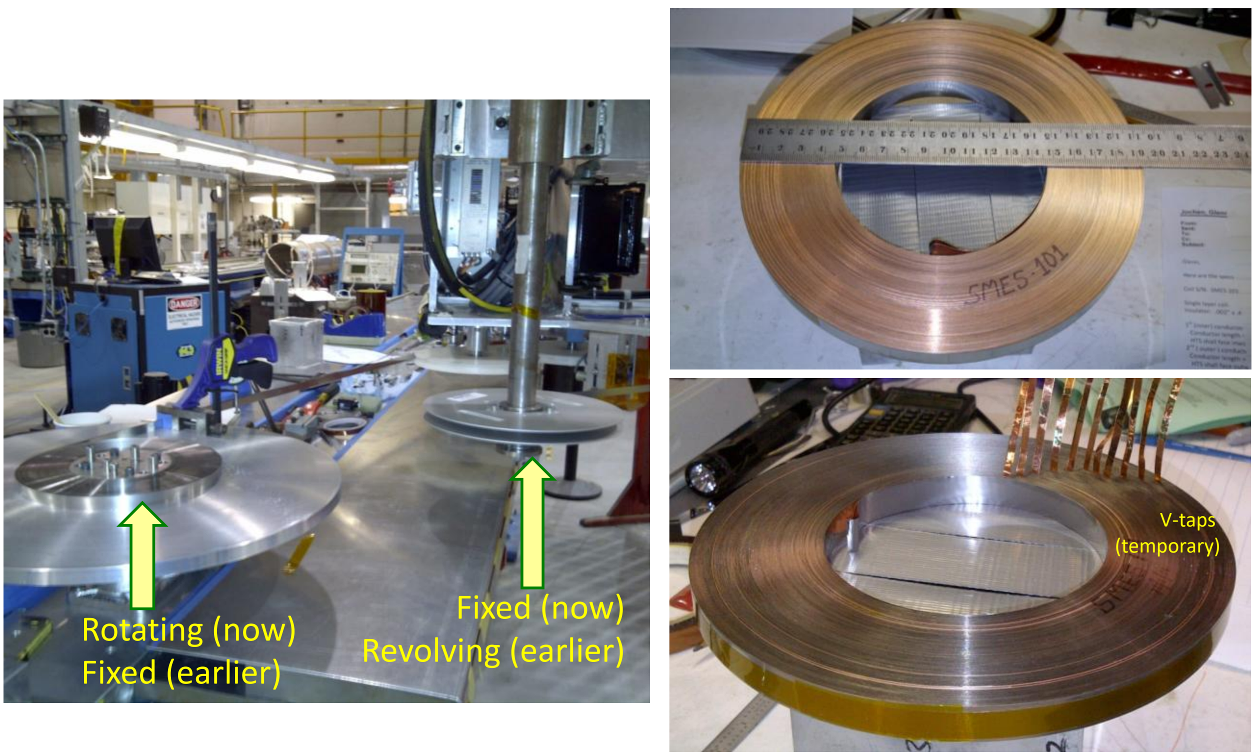

Fig. 6: Updated coil wind machine (left side) and two sides of a coil (right side) wound with this machine. Bottom part of the picture on the right shows the side with a number of voltage taps.

Test Results of Splice Joint

Splices are often one of the most critical parts of the magnet construction. R&D on developing advanced low resistance splice joint is being performed by Advanced Energy Material (AEM) group. The results of that research will be available later and are expected to be used in future coils. Since splices are required to construct the coils to meet Q6 Go/NoGo milestone, for now we adapt the techniques based on previous experience with joints in Superconducting Magnet Division (SMD).

First step is to determine the length that must be used in making the joint. Experimental joints of several lengths were built and tested. Fig. 7 (top) shows a typical joint in a test fixture. Measured joint resistance as a function of overlap length is plotted on the left and as a function of 1/Area on right. Based on these measurements, it is determined a 15 cm length of joint should be acceptable for these joints for which we already have a fixture. The measured joint resistance of ~2.1 nano-ohms is below the project goal of 5 nano-ohms. This value, measured at 77 K, will get reduced further due to lower operating temperature (~4 K) but will increase in presence of field. However, the splice resistance based on this construction technique is still expected to remain well below the project goal of 5 nano-ohms.

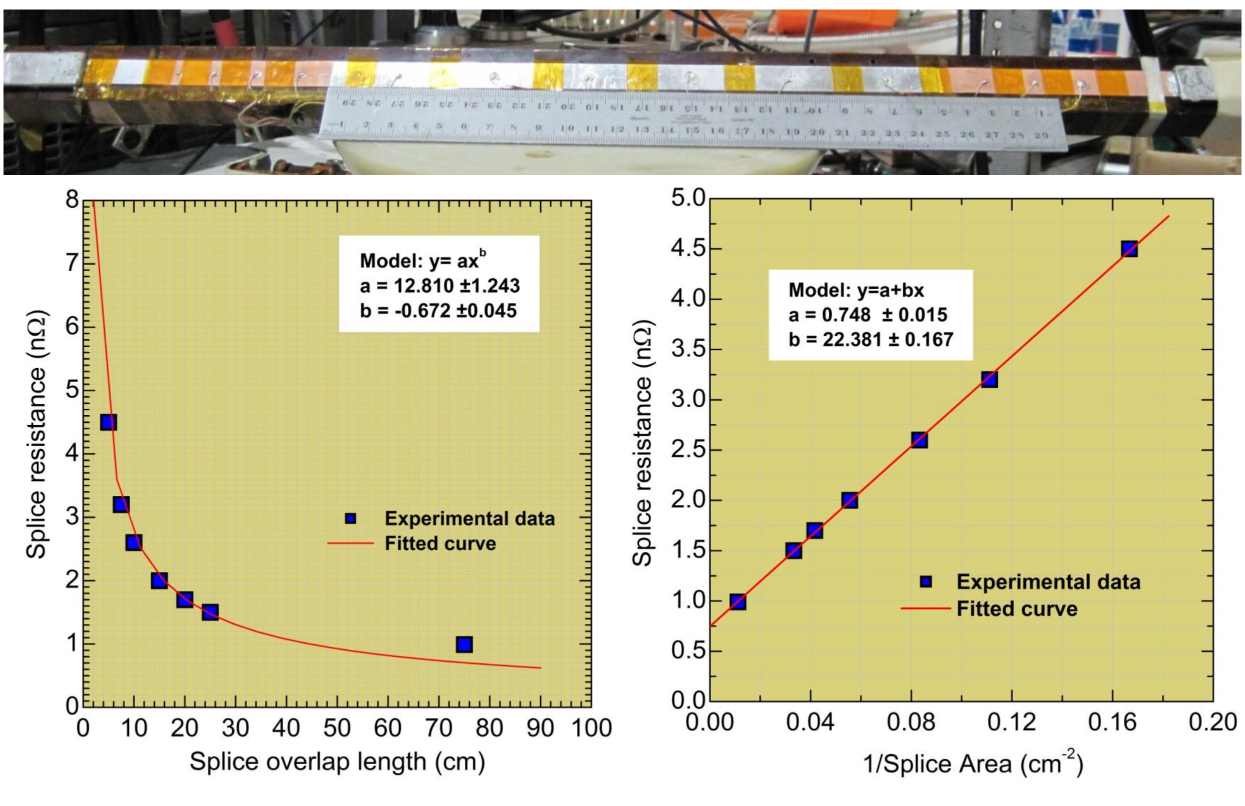

Fig. 7: A comprehensive summary of the test results of several joints built and tested as a function of splice overlap length. A typical joint in a test set-up is shown on top. Measured joint resistance as a function of overlap length is shown on left and as a function of 1/area on right.

It may be noted (see Fig. 7) that we were able to make a joint with less than 1 nano-ohms resistance at 77 K, self-field. Examination of fitting (see Fig. 7, right) shows that irrespective of the length of this splice, the limit of this technology is about 0.7 nano-ohms.

The splice joints described so far have been built and tested in straight geometry. The joint will, however, be bent in coil with a radius depending on the location of joint. There is a potential for a degradation of joint due to this bending. To determine bending degradation, if any, we measured the joint resistance before and after bending. The minimum bend diameter of the joint in coil will be significantly more than the 100 mm (coil inner diameter). For example, a joint after 50 meter of wire in coil will have a bend diameter of over 140 mm. We performed the measurement of bending degradation at 114 mm diameter using an existing fixture. Since the bending degradation of the joint remains small even at this small diameter then the degradation will not be of concern in the coil we are making.

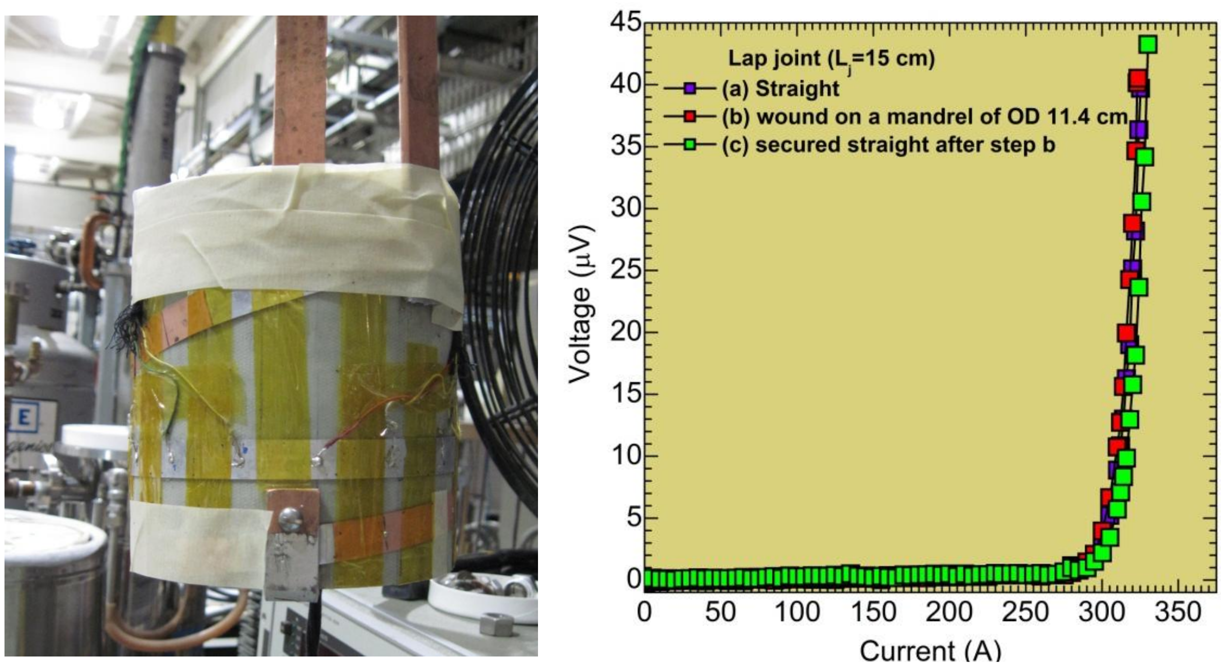

Fig. 8: Fixture to measure bending degradation of splice joint is shown on the left and measured performance of joint as a function of current at various steps is shown on right. The performance is tabulated at the bottom of the above figure.

Table 2 : I_c, n value and resistance (R_j) of lap joint sample under the following three experimental conditions. The experiments were carried out at 77 K in self-field condition.

	Experimental condition	I_c (A)	N	Rj (nΩ)
a	Straight sample	325.8	26.8	2.05 ± 0.04
b	Wound on a mandrel (bend diameter = 114 mm)	324.7	26.6	1.79 ± 0.04
c	Unwound and secured on a straight sample holder after step b	324.5	26.3	1.82 ± 0.03

The fixture used to make these bending degradation measurements is shown in Fig. 8 (left). The slope of the line in the straight region of the plot in Fig. 8 (right) gives the joint resistance and the polynomial fit of the increasing voltage region gives the n-value. The performance of the joint at various steps of this experiment is tabulated in Table 2. One can see that there is practically no degradation even at a diameter of 114 mm. A small decrease in joint resistance may be attributed to either measurement uncertainties or the influence of slightly increased pressure during the experiment.

Most of the measurements discussed in this section were carried out at 77 K. The proposed high field SMES coil, however, will operate at 4 K where the joint resistance will be lower. We have carried out an experiment to measure this decrease in joint resistance. Fig. 9 shows these measurements along with the fixture used. The measured resistance of this ~50 mm long splice joint decreased from 4.5 nano-ohms to 3.35 nano-ohms - a ~26% reduction in value.

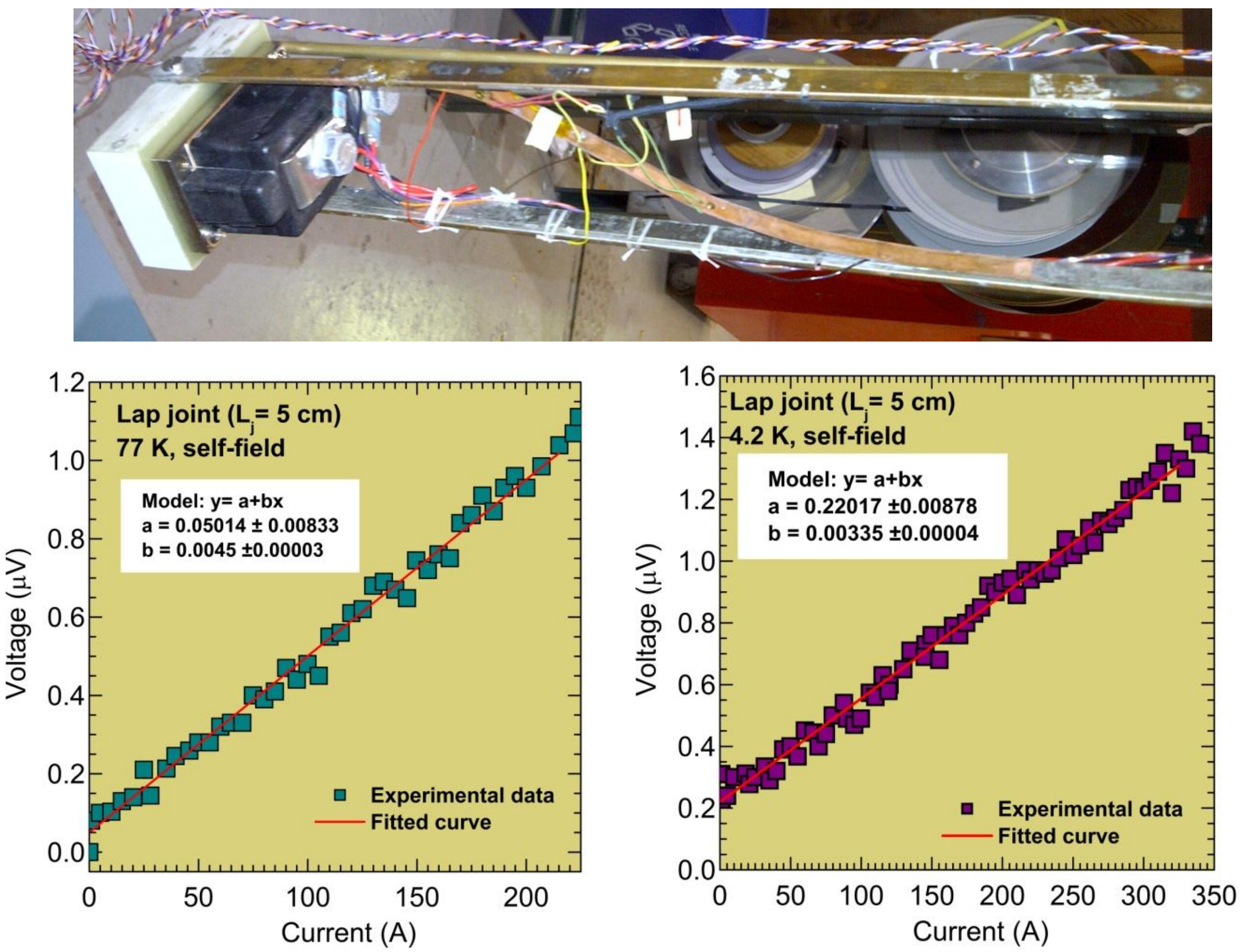

Fig. 9: A comparison of the performance of joint at ~77 K and ~4 K. The test set-up is shown on the top. The measured performance as a function of current is shown on left at ~77 K and on right at ~4 K. The value of joint resistance decreases from 4.5 nano-ohms at ~77 K to 3.35 nano-ohms at ~4K.

Quench Protection

The basic unit of quench protection system was previously tested in a small two mini pancake coil fixture during the last quarter. The desired sensitivity for voltage detection is 1 mV in presence of noise in the presence of a large inductive voltage. We continue to make progress in implementing this basic unit in a larger system involving many more coil sections (about fifty six) producing a large energy storage system. To help develop overall quench protection system, we continue to analyze results of previous high current test at 4 K. One such detailed analysis is shown in Fig. 10. This shows a typical behavior during and soon after the quench. This particular case is for storage at 614 A in conditions similar to that faced by an individual coil in the complete system. 21 K temperature was chosen to bring coil closer to the quench threshold. One can see (left) that current drops rapidly to help protect the coil from the quench or from a forced shut-off. The schematic of the protection circuit is shown in right.

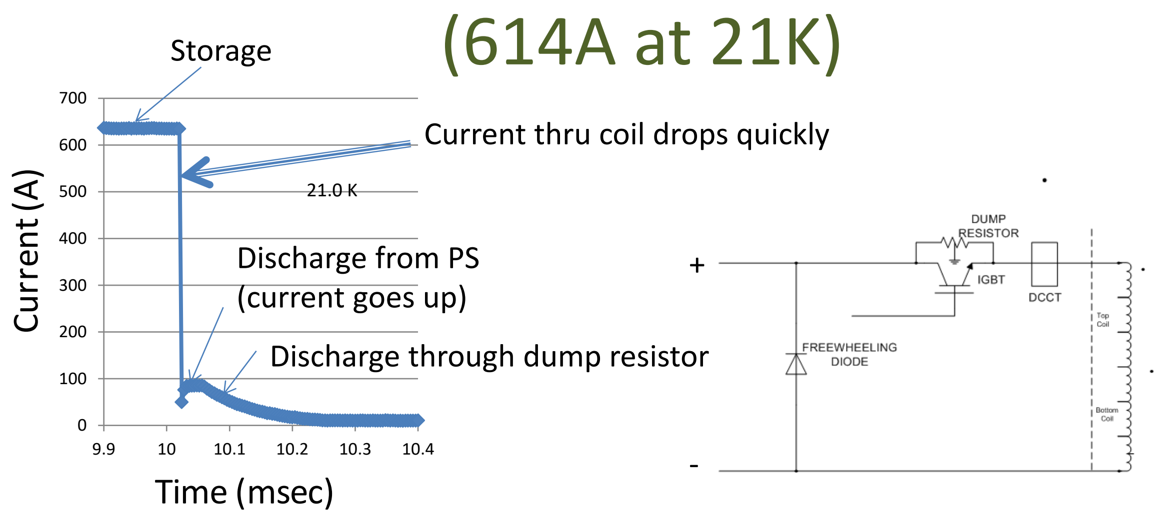

Fig. 10: A typical behavior of coil during quench where the current discharge is analyzed (above case is for discharge at 614 A). The basic circuit is shown schematically in right section and the overall discharge in left section.